

# THE EUROPEAN SPALLATION SOURCE

S. Peggs\*, ESS, Lund, Sweden  
for ESS/AD and the ESS/ADU Collaboration

## Abstract

Lund was chosen as the site for the European Spallation Source (ESS) in 2009, and a company, ESS AB, was created to design, build and operate it. In 2010 the Accelerator Design Update (ADU) collaboration was formed to update the design that was established in 2003, and to deliver a Technical Design Report at the end of 2012 [1]. Detailed planning for the Prepare-to-Build prototyping project has begun, and potential future power upgrades are being considered. First protons are expected in 2018, and first neutrons in 2019 [2].

The updated design delivers 5 MW of 2.5 GeV protons to a single target, in 2.86 ms long pulses with a 14 Hz repetition rate. The linac will have a normal conducting front end with an ion source, a Radio Frequency Quadrupole (RFQ), and a Drift Tube Linac (DTL). The superconducting section of the linac contains spoke cavities followed by two families of elliptical cavities [3]. The ESS has the ambitious goal of being a sustainable research facility with zero release of carbon dioxide [4]. This will be achieved through a combination of actions, with a focus on the linac – the most energy hungry component. Care is being taken to optimize the overall energy efficiency, and to re-use the hot water coming out of the facility.

## INTRODUCTION

Spallation is the nuclear process that emits neutrons at a spectrum of energies after highly energetic particles bombard heavy nuclei – for example, when the ESS proton beam strikes a rotating tungsten disk target. These neutrons are cooled in moderators adjacent to the target, before being transported of order 100 m through neutron guides to experimental instruments [5].

The neutron time-of-flight, and therefore individual neutron energies, are readily measured at pulsed sources like the Spallation Neutron Source (SNS) and the ESS. The SNS combines a full energy superconducting linac with an accumulator/compressor ring to provide high intensity short pulses ( $\sim 1 \mu\text{s}$ ) of protons to a mercury target. The ESS avoids the need for a costly and performance-limiting ring, by delivering even higher intensities to experiments that are capable of using long pulses ( $\sim 3 \text{ ms}$ ) [6]. Long pulse implementations also permit  $H^+$  operation, maintaining relatively low peak currents, and enabling small emittances and apertures in all beamlines.

It is generally agreed that a kinetic energy of 1–3 GeV is optimal for practical target and moderator designs, and in order to keep the shielding requirements reasonable. The

ESS energy of 2.5 GeV enables an average macro-pulse current of 50 mA that is consistent with the need for high reliability, but still leaves some leeway for a potential energy (and thus power) upgrade. The current limit is mainly set by space charge effects at low energy, by the power that can be delivered to the beam in each cavity at medium and high energies, and by beam losses.

Table 1: High level ESS parameters.

Parameter	Unit	Value
Average beam power on target	MW	5.0
Proton kinetic energy on target	GeV	2.5
Average macro-pulse current	mA	50
Macro-pulse length	ms	2.86
Pulse repetition rate	Hz	14
Number of instruments		22
Number of target ports		50
Reliability	%	95
Maximum average beam loss rate	W/m	1.0
RF frequency: RFQ, DTL, spokes	MHz	352.21
RF frequency: elliptical cavities	MHz	704.42

## LAYOUT

The accelerator achieves the high level parameters listed in Table 1 using the schematic “2011 hybrid” baseline layout shown in Figure 1, in which the linac is optimized for 50 mA operation with a single cavity per klystron [7, 8]. High level parameters (such as the 5 MW beam power) are rigidly fixed, while some lower level parameters are subject to modest evolution. Live parameters, continuously maintained and under configuration change control, are publicly available on-line [9, 10]. Layout changes in the last year were influenced by factors like the geometry of the cryomodules, the maximum gradient in the cavities, and the choice of phase advance in the superconducting linac. Lattice parameters exist in piecemeal form, from the partners in the ADU collaboration. Complete integration into a single end-to-end lattice is scheduled for the autumn of 2011.

**Proton source.** There is no need for charge exchange injection (into an accumulator ring) for a long pulse source, so the ESS ion source will produce a proton beam. The source will be a compact Electron Cyclotron Resonance source similar to the VIS source [11] in Catania, and the SILHI source [12] at CEA-Saclay.

**LEBT and RFQ.** Beam is transported from the ion source through the LEBT to the RFQ, for bunching and

\* steve.peggs@esss.se

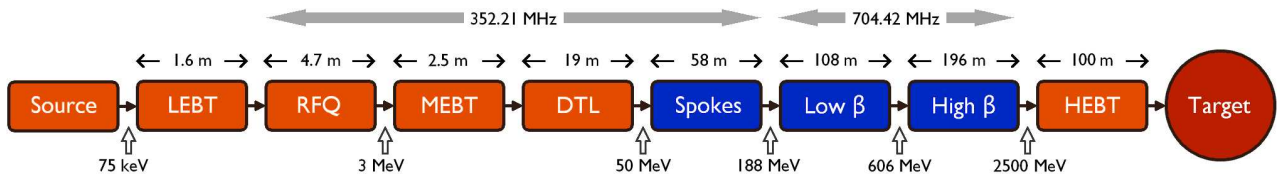


Figure 1: The “2011 hybrid” baseline layout of the ESS linac. Red sections – the RFQ, the DTL, and the Low-, Medium- and High- Energy Beam Transports, (LEBT, MEBT, and HEBT) – are normal conducting. Blue sections – spoke resonators, low- $\beta$ , and high- $\beta$  elliptical cavities – are superconducting.

Table 2: Structures in the “2011 hybrid” linac layout.

Parameter	Unit	Value
Number of DTL tanks		3
Number of spokes per spoke cav.		2
No. of spoke cavs per cryomodule		2
Number of cells per elliptical cav.		5
No. of low beta cavs per cryomod.		4
No. of high beta cavs per cryomod.		8
Number of spoke cryomodules		14
Number of low beta cryomodules		16
Number of high beta cryomodules		15
Geometric beta, spoke resonators		0.57
Geometric beta, low beta cavities		0.70
Geometric beta, high beta cavities		0.90
Operational voltage, spokes	MV	6.0
Operational voltage, low beta	MV	10.5
Operational voltage, high beta	MV	18.5
Expected gradient, low beta, horz.	MV/m	15
Expected gradient, low beta, V test	MV/m	17
Expected gradient, high beta, horz.	MV/m	18
Expected gradient, high beta, V test	MV/m	20
Elliptical coupler power, to beam	MW	1.2

acceleration up to 3 MeV. The four vane type RFQ will be able to accelerate up to 100 mA of protons from the ion-source voltage of 75 kV to 3 MeV [13]. A first test run of the RFQ under realistic ESS conditions will be performed at the IPHI RFQ, which is presently under commissioning at CEA-Saclay in Paris.

**MEBT and DTL** The MEBT transports beam from the RFQ and matches it into the first DTL tank [14]. There is active discussion on whether or not the MEBT will contain a fast chopper [15]. There will be a chopper in the LEBT or in the MEBT, or possibly in both, to define the time structure of the beam. Rise and fall times in the range 0.1–1  $\mu$ s are envisaged. The MEBT will also contain collimators to reduce beam losses further down the linac, and to produce a well defined beam distribution that is more easily modeled and understood. The DTL design derives from the Linac4 design, at CERN.

**Spoke resonators.** The transition to superconducting structures occurs after the DTL at 50 MeV, when the beam

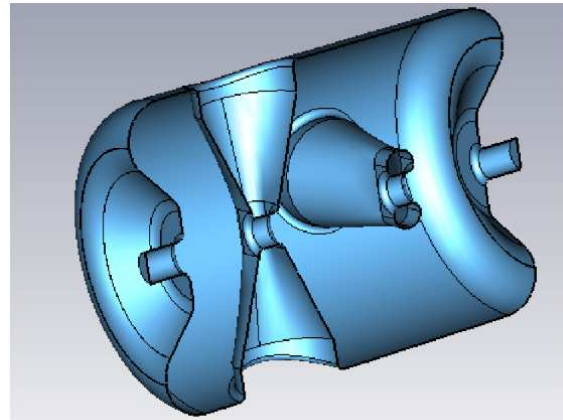


Figure 2: Double spoke resonator cavity, with an accelerating gradient of 8 MV/m and a geometric  $\beta$  of 0.57.

enters double spoke resonator cavities as shown in Figure 2. The ESS will be the first major accelerator to use spoke cavities, which have the advantages of large longitudinal and transverse acceptances, individual tunability that leads to resilience to single-cavity failures [16], and a large inherent mechanical stiffness that reduces the sensitivity to microphonics and to Lorenz force detuning. Recent tests at Fermilab [17] (without beam) demonstrated accelerating gradients significantly in excess of the 8 MV/m proposed for ESS. Excitation of HOM power by the passage of the beam remains a topic of concern and study [18].

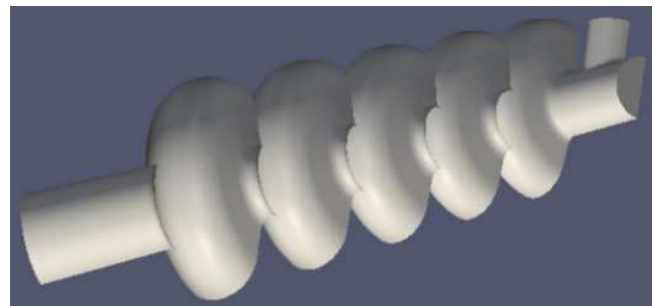


Figure 3: Elliptical cavity, with a high geometric  $\beta$  of 0.90.

**Elliptical cavities.** The frequency doubles to 704.42 MHz at the entrance to the first of two families of elliptical 5-cell cavities, with geometric betas of 0.70 and 0.90. The second family of 15 high-beta

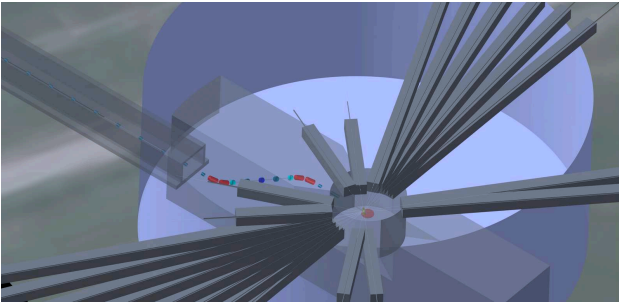


Figure 4: Interface between the HEBT, the rotating tungsten disk target, moderators, and the 22 neutron beamlines.

cryomodules, each with 8 cavities, delivers about 75% of the total proton energy, from 600 MeV to 2.5 GeV. The cavity geometry shown in Figure 3 includes only the fundamental power coupler. The option of adding a HOM coupler to extract HOM power is under active discussion.

**HEBT, target and neutron beamlines.** Figure 4 shows the HEBT rising vertically 10 m (with no horizontal bend) out of a FODO channel into a target that sits 1.6 m above ground level. The uphill straight is available for momentum and betatron collimation. The solid rotating tungsten target is cooled by helium gas. Specifications of the size and intensity distribution of the beam on the target are under discussion. The power dissipation and distribution on the proton-beam window (separating the linac vacuum from the target atmosphere) are also under study. Not shown in Figure 4 is the straight-ahead tune-up dump that receives beam when the vertical dipoles are turned off. The design of the beam flattening and the HEBT as a whole is being elaborated by the Århus group [19, 20, 21].

## HYBRID CRYOMODULES

Superconducting linacs typically have continuous (eg XFEL) or segmented (eg SNS) cryostats. A continuous cryostat has a lower static heat load on the cryogenic plant, reducing energy consumption and operational costs. Each segmented cryomodule has its own insulation vacuum, and requires jumper connections to an external cryogenic distribution line. A segmented design is more serviceable, since individual cryomodules can be valved off, warmed, and repaired or exchanged. Further, beam instrumentation can be placed in the warm spaces between segmented cryomodules. Beam instrumentation is in general more challenging for a  $H^+$  linac than for an  $H^-$  linac. For instance, it would require a significant R&D effort to develop a beam-profile monitor that operates efficiently at 2 K [22, 23, 24].

The current ESS baseline adopts a hybrid design, in which a cold interconnect between neighboring cryomodules is enclosed by a sleeve that is cooled to the intermediate temperature of the outer thermal screen of the main cryostats, about 70 K. This reduces the heat load and permits some of the interconnects to be left at room tempera-

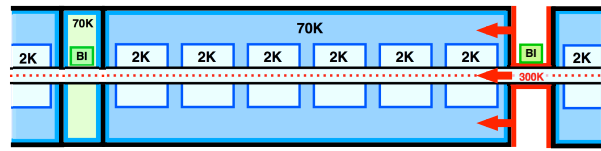


Figure 5: Interconnects between hybrid cryomodules may be either warm or cold ( $\sim 70$  K).

ture, as shown in Figure 5. This hybrid scheme is mechanically more complex than a simple segmented design. Its relative advantages and disadvantages are under evaluation.

## BEAM PHYSICS

**Optics.** Figure 6 (top) shows transverse beta functions that increase along the length of the linac, driven by doublet quadrupoles that weaken as the proton energy increases. The transverse RMS beam size remains approximately constant, with very little emittance growth. Figure 6 (bottom) represents the longitudinal optics by the phase advance per cryomodule, driven by the longitudinal cavity strengths recorded (indirectly) in Figure 7.

Figure 7 records the RF power sources requirements for a smooth acceleration transition between the different families of superconducting structures. The linac will be powered by one klystron per superconducting cavity, plus one for the RFQ, and (1,2,2) for DTL tanks (1,2,3). This gives maximum flexibility for beam tuning and robustness against faults – the linac can be retuned to operate after the failure of any individual SC cavity [16]. The power sources are gradient-limited rather than power-limited at 50 mA beam current [25], but with only a modest margin.

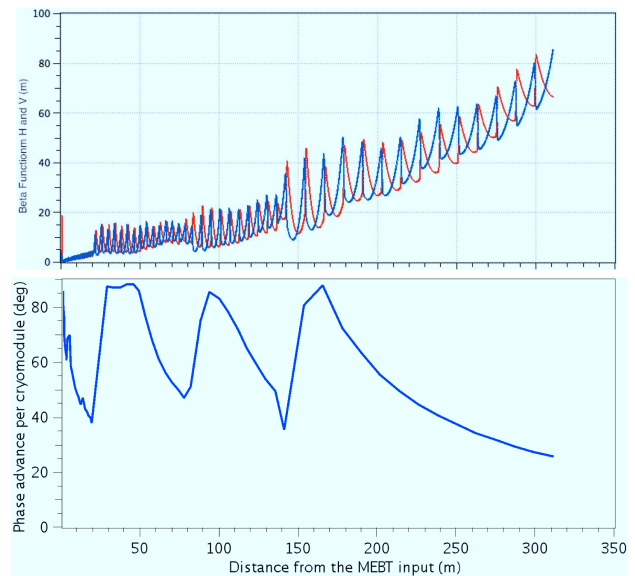


Figure 6: Transverse beta functions (top) and the longitudinal phase advance per cryomodule (bottom), for most of the ESS linac.

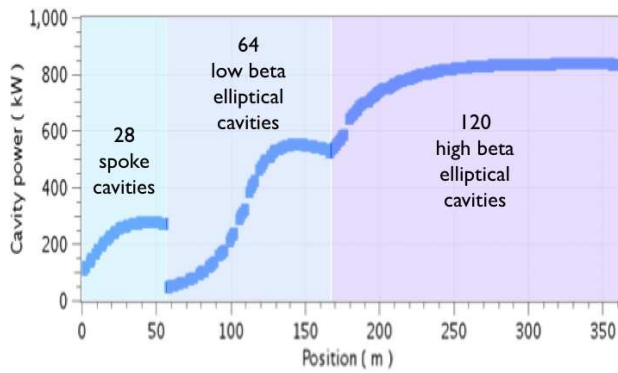


Figure 7: The power to beam of the superconducting part of the linac [26], as calculated from the lattice in [27].

**Simulations and beam losses.** Beam-dynamics simulations show that the transverse acceptance of the superconducting linac is an order of magnitude larger than the RMS emittance of the beam in an ideal linac, and also substantially larger than the envelope given by the outermost particles [28, 29]. Longitudinally, the acceptance is two orders of magnitude larger than the RMS emittance.

Excessive radio-activation from beam losses larger than about 1 W/m would hinder hands-on maintenance. Beam losses from aperture limitations, transition regions and misalignment are readily simulated, yielding mechanical tolerances for cavity designs, supporting infrastructure and other equipment. Intra-beam stripping is plausibly an important source of beam losses in  $H^-$  linacs like the SNS, but not in the  $H^+$  ESS [30]. Other beam loss sources are Hoffman space charge resonances [31], transverse overfocusing [32], and uncollimated low energy beam halo. Attaining the ability to confidently predict the relative importance of loss mechanisms is a fundamental challenge to our ability to design multi-MW proton linacs.

## RADIO FREQUENCY SYSTEMS

**RF frequency.** Lower frequencies are favored at lower energies due to relaxed manufacturing tolerances in cavity components, and to the capacity for large beam apertures. They also increase the transverse focusing strength of RFQs, reduce RF losses in cavities, and mitigate HOM effects. Higher frequencies decrease the cavity size, making them easier to handle and reducing manufacturing costs, and also reduce the cryogenic envelope and power consumption with superconducting structures. A frequency of 600–800 MHz is a good compromise for elliptical structures like the CERN Superconducting Proton Linac and the ESS, which both share frequencies of 352.21 MHz and 704.42 MHz, at low and high energies [33, 34].

**RF power distribution.** Special care has to be taken with the design of the RF power sources, distribution system and controls [35], due to severe space limitations, reliability and safety concerns and high investment and opera-

tional costs [36]. The ESS design goal of being a sustainable research facility requires the minimization of power consumption, and the re-use of all heat from cooling water. The entire facility is divided into different categories, depending on the cooling needs and the temperature range for reliable equipment operation. The highest temperature zones will be the RF loads, circulators, compressors, and the klystrons collectors, according to SNS experience. Higher temperature operation of these systems permits the temperature of the cooling water leaving the facility to a value ( $> 70$  C) that enables re-sale to the district heating system of the local community.

**Higher Order Modes.** High energy efficiency requires superconducting RF structures with very high quality factors. Consequently, each HOM tends to have a long damping time, with a significant risk that it will still be active when the next macro-pulse arrives. It has been shown [37] that HOMs may harm high power proton beam quality, primarily if HOMs are strongly coupled with the frequency content of the beam. HOM excitation and decay must be very well understood and, if necessary, suppressed, in order to avoid disrupting longitudinal phase space, perhaps causing beam loss beyond the 1 W/m limit [38]. If necessary, the ESS will remove HOM power using couplers placed at cavity locations where the more destructive parasitic modes have large amplitudes, rather than lossy material around the beam pipe between neighboring cavities. HOM couplers can also be instrumented to measure the 4D transverse location of the beam [39]. Ongoing beam dynamics studies will form an important part of the decision on whether or not to install HOM couplers [40].

**Field Emission & MultiPacting.** SNS experience indicates that FE & MP could significantly limit the performance of the ESS elliptical cavities [41]. FE electrons lost on the cavity walls increase the load on the cryogenic system, and decrease the quality factor of the cavity. FE electrons may also thermal detune the notch filter used to reject the accelerating mode from the HOM coupler (if present), causing excessive power to be coupled out into the HOM electronics. Further, excessive MP could quench cavities, and could disrupt longitudinal phase space. The FE/MP phenomena that cause problems at SNS are particularly complex. Several different simulation-based calculations have commenced, on individual couplers, full cavities, and multiple cavities [42].

**Low Level RF.** RF stability is particularly important in proton linacs, because the semi-relativistic velocities cause phase and amplitude errors in one cavity to alter beam arrival times in downstream cavities. These errors accumulate along the length of the linac. Investigations of phase and amplitude errors due to modulator ripple and droop have begun [43, 44]. Proportional and proportional-integral (PI) controllers are being studied for the normal-conducting and superconducting cavities.

## POTENTIAL UPGRADES

Different upgrade strategies available to the ESS are under discussion, within the constraint of a single target station [45]. Short pulse operation with  $H^-$  beam is not under consideration. In general, the ESS baseline design is optimized for 5 MW, but may incorporate features providing upgrade potential, so long as their day-one inclusion is inexpensive. Thus, the target monolith is equipped with 50 neutron beam ports, providing a potential path towards a total of 44 experimental instruments. Similarly, provision may be made for parasitic proton extraction lines, and also for a power upgrade.

Superficially, a power upgrade to 7.5 MW “just” requires raising the average beam current to 75 mA. However, the ESS design, optimized for 50 mA, could be difficult or inefficient to operate at higher currents, for example due to mismatching between the RF coupler and the beam loaded cavity, and due to HOM effects. Upgrades to larger beam currents would require upgraded RF power sources, or reduced accelerating voltages. Increasing the current of the proton beam would also require redesigning the front end, including the ion source.

The beam power could also be increased by raising the proton beam energy, or the repetition rate. The 14 Hz repetition rate is intimately linked to instrument design and location, and is very difficult to change. Either an energy upgrade or a current upgrade – or a judicious mixture of the two – would require additional acceleration cavities unless the RF power sources are changed.

Any power upgrade would also require the target, its cooling, and shielding to be redesigned. An energy upgrade must also take into account the higher energy target conditions. For example, the centre of neutron production would move a few centimetres if the energy increased from 2.5 GeV to 3.0 GeV. However, a pure energy upgrade using additional accelerating structures would have little influence on beam dynamics and would not require any major modification of the existing linac.

## CONCLUSION

The on-going Accelerator Design Update project will result in a Technical Design Report with associated costing and scheduling at the end 2012. It will also produce interface and requirement documents for the next project, “Prepare-to-Build” (P2B), which will deliver all manufacturing specifications and detailed integration plans in a timely fashion. P2B will also permit orders to be placed, and allow testing and construction and assembly to begin, so that protons can be delivered to the target station in 2018. These projects are being performed in a collaboration between European universities and institutes with important contributions from overseas laboratories and universities.

## REFERENCES

[1] C.Oyon, these proceedings, WEIB05.

- [2] T.Hansson et al, these proceedings, WEPC166.
- [3] G.Devanz, these proceedings, TUZB01.
- [4] C.Carlike, these proceedings, THEA01.
- [5] B.Willis & C.J.Carlike, Oxford University Press, ISBN 978-0-19-851970-6, 2009.
- [6] F.Mezei, J. Neutron Research 6 3-32, 1997.
- [7] H.Danared, these proceedings, WEPS059.
- [8] M.Eshraqi, these proceedings, WEPS060.
- [9] <http://esss.se/linac/Parameters.html>
- [10] K.Rathsman et al, these proceedings, TUPS096.
- [11] S. Gammino et al, ECRIS10, MOPOT012, 2010.
- [12] R.Gobin et al, Rev.Sci.Instr 73, 2002.
- [13] R.Ainsworth et al, these proceedings, MOPC049.
- [14] I.Bustinduy & J.L.Munoz, these proceedings, WEPC022.
- [15] C.Plostinar et al, “Chopping options for ESS”, unpublished, 2011.
- [16] M.Eshraqi, these proceedings, WEPS063.
- [17] R.Madrak et al, LINAC10, THP031, 2010.
- [18] M. Lindroos, ESS AD Tech Note ESS/AD/0010, 2010.
- [19] H.Danared, ESS AD Tech. Note ESS/AD/0008, 2011.
- [20] A.Holm et al, these proceedings, THPS050.
- [21] H.Thomsen et al, these proceedings, THPS031.
- [22] A.Jansson & L.Tchelidze, DIPAC11, MOP184, 2011.
- [23] A.Jansson et al, PAC11, TUPD02, 2011.
- [24] L.Tchelidze & A.Jansson, these proceedings, TUPC131.
- [25] M.Eshraqi et al, these proceedings, WEPS062.
- [26] K. Rathsman et al, ESS AD Tech Note ESS/AD/0020, 2011.
- [27] M. Eshraqi, ESS AD Tech Note ESS/AD/0007, 2011
- [28] A.Ponton, these proceedings, MOPS039.
- [29] M.Eshraqi & H.Danared, these proceedings, WEPS061.
- [30] V. Lebedev et al, LINAC10, THP080, 2010.
- [31] I.Hofmann & K.Beckert, IEEE TNS. NS-32, 2264, 1985.
- [32] Y.Zhang et al, PRST-AB 11, 104001, 2008.
- [33] F.Gerigk et al, CERN-AB-2008-064, 2008.
- [34] M.Harrison et al, “ESS Frequency Advisory Board Report”, 2010.
- [35] I.Verstovsek et al, these proceedings, THXA01.
- [36] K.Rathsman et al, these proceedings, MOPC136.
- [37] M.Schuh et al, PRST-AB 14, 051001, 2011.
- [38] C.Welsch et al, these proceedings, MOPS082.
- [39] S.Molloy et al, PRST-AB 9, 112802, 2006.
- [40] S.Molloy et al, these proceedings, MOODB02.
- [41] I.Campisi et al. PAC07, WEPMS076, 2007.
- [42] S.Molloy et al, these proceedings, MOPC050.
- [43] R.Zeng et al, ESS AD Tech Note ESS/AD/0011, 2011.
- [44] A.J.Johansson & R.Zeng, these proceedings, MOPC161.
- [45] M.Lindroos et al, these proceedings, WEPS064.